Получение, структура, свойства

D. Meng, W. Yue*, F. Lin, C. Wang, Z. Wu (Beijing, China)
*cugbyw@163.com, yw@cugb.edu.cn

Thermal stability of ultrahard polycrystalline diamond composite materials

Thermal stability of the ultrahard polycrystalline diamond (UHPCD) composite material developed by the reinforcement of the polycrystalline diamond (PCD) with chemical vapor deposition (CVD) diamond has been investigated in a flow of argon at 1200 °C. The indentation, Raman spectra and wear test have been performed to compare hardness, C–C structure and wear resistance of untreated and thermal treated UHPCD. It has been shown that the hardness of CVD diamond in UHPCD attains 133±7 GPa after high pressure and high temperature, while after thermal treatment the hardness decreases to 109±3 GPa, and the wear resistance of the thermal treated UHPCD decreases from 0.17 to 0.6 mg/km. The narrowing of full width at half maximum and shift of Raman peak to lower frequencies of CVD diamond in thermal treated UHPCD imply a decrease of crystal structural defects and compressive stresses, which results in a drop of the hardness of CVD diamond in a thermal treated UHPCD. The higher wear rate of thermal treated UHPCD is due to the lower hardness.

Keywords: *ultrahard polycrystalline diamond, thermal stability, CVD diamond, wear resistance.*

INTRODUCTION

Generally, polycrystalline diamond (PCD) materials are used as cutting inserts in drilling bits. The performance and service life of drilling bits are usually determined by mechanical properties of PCD. It is well known that PCD with extensive diamond–diamond bonding can be synthesized under high pressure and high temperature (HPHT) by using metallic powders as sintering agents. However, a large amount of metallic agents in the PCD could cause deterioration such as graphitization or cracking above about 700 °C [1, 2]. Therefore, the working temperature of sintered diamond has been limited to 700 °C.

To synthesize PCD with a high thermal stability, an alternative approach is to use unconventional non-metallic sintering agents such as calcium carbonate and magnesium carbonate. Akaishi et al. [3] investigated the behavior of magnesium carbonate ($MgCO_3$) as sintered agent at 7.7 GPa and 1800–2450 °C in a belt press [3]. PCD sintered with $MgCO_3$ showed no drop of Vickers hardness until after a

heat treatment above 1300°C for 30 min in a vacuum of $1 \cdot 10^{-3}$–$1.5 \cdot 10^{-3}$ Pa. Westraadt et al. reported the synthesis and characterization of PCD sintered with $CaCO_3$ at 8±0.5 GPa and 2000–2200 °C in a 6–8 Kawai type multianvil high pressure apparatus [4]. No wear resistance reduction of PCD was detected after a heat treatment to 1200°C in vacuum ($5 \cdot 10^{-3}$ Pa) for 30 min in a machining test on a silica resin bar. However, because of the limitation of extremely high pressure and high temperature conditions, only a few of carbonate sintered PCD toward has been applied in industrial field.

Shulzhenko et al. [5] reported a new approach to sintering superhard material named the ultrahard polycrystalline diamond (UHPCD) composite material. The basis for manufacturing the UHPCD was a combination of the high-pressure technique and chemical vapor deposition (CVD) method. Superior hardness and excellent wear resistance are the main features of UHPCD. The hardness of the CVD diamond in UHPCD is as high as 140 GPa, which is higher than that of natural diamond single crystal. The hardness of PCD in the UHPCD is about 50 GPa. The wear resistance of the hybrid UHPCD in turning granite of the XI drillability index is higher than that of PCD by a factor of 14. Shulzhenko et al. [6] investigated also a thermal stability of the PCD material. It was found that the PCD retained hardness 23 GPa at a temperature of 1200 K, while the initial hardness was 44.8 GPa. However, the thermal stability of the UHPCD has not been studied.

In this study, the thermal stability of the UHPCD was investigated at 1200 °C in flow of argon. It contrasted the hardness, wear performance and Raman spectrum of the UHPCD before and after thermal treatment. The mechanism of the decreased mechanical properties of the CVD diamond in thermal treated UHPCD was further discussed.

EXPERIMENTAL

Materials

A diamond micron powder and CVD diamond were used as the raw materials. The diamond powder had grains of sizes from 20 to 30 μm. The CVD diamond with a size of 0.8×0.8×4 mm was produced by a deposition in the microwave frequency plasma in methane–hydrogen mixtures. The UHPCD samples were sintered by the same method as in the previous report [5]. The UHPCD samples (4 mm in diameter and 4.5 mm high) were chemically purified to remove graphite residues. The optical image of UHPCD is shown in figure. The characteristic feature of the UHPCD is a reinforced CVD diamond surrounded by PCD.
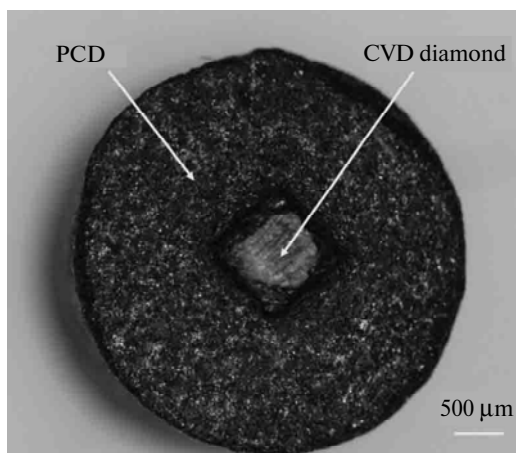
Optical image of UHPCD.

Characterization

The UHPCD sample was heated to 1200 °C in argon for 10 min. After that, the sample was cooled to room temperature under argon flow. The weight loss was calculated from the weight of the sample before and after the thermal treatment.

The hardness of the CVD diamond was determined using a PTM-3 microhardness tester with a Vickers diamond pyramid as an indenter. The hardness value was found by the generally accepted formula $H_V = 1.8544P/d^2$, where P is the indentation load, d is the arithmetical mean of two diagonals of the indent. The measurements were performed under loads of 4.9 and 9.8 N. The indent diagonals were measured using a Neophot optical microscope.

The chosen indentation loads may be considered optimal, as in using both of them the obtained hardness values were practically the same, and in addition, during the indentation no fracture of the tested material was observed. During the hardness measurements, a particular attention was paid to the state of the diamond pyramid tip, which was assessed by measuring indents on the polished surfaces of standard specimens with the hardness of about 4 GPa. After each three measurements of the tested samples, an indent was made on the standard specimen, and the sizes of the diagonals of the indents on tested samples were compared to those made on the standard specimen by the diamond pyramid after production. In the case that the sizes of the indent diagonals deviated from the initial value by more than 3 %, the diamond pyramid was corrected. No fracture of the indenter was observed during the hardness measurements under the indentation loads used.

The Raman spectra were measured using a Horiba Jobin Yvon T64000 spectrometer equipped with an Olympus BX41 confocal microscope. A discrete emission line of an Ar–Kr laser (λ_{exc} = 514.5 nm) was used as the source of the optical excitation. The laser beam was focused onto a sample at a site 0.2–0.5 μm in diameter. The space spectral mapping of the sample was conducted by displacing automated table at a step of 0.1 μm. The frequency of the spectral line was accurate to 0.15 cm^{-1}. The Raman spectra were measured in the center of the CVD diamond samples.

The wear tests were conducted in cutting Korostyshev granite of the XI drillability category on a special stand based on a DIP-200 screw–cutting lathe. The Korostyshev granite is characterized by stable properties, high hardness, and abrasivity. During the tests, a special equipment as a split cylinder and a sleeve for fixing the rock core as well as a special workholder to fix the sample of a rock destruction element in the machine toolholder (based on a drill chuck) were used.

The rock sample was fixed in the chuck of the special workholder, approached to the rock core surface and was longitudinally cut at a set penetration depth.

To measure the wear loss of samples during the tests a Sartorius type balance was used. The cutting parameters: rotation frequency – 355 r/min; penetration depth – 0.25 mm. Parameters that were registered: deepening in penetration with an accuracy of 0.05 mm; turning time accurate to 1 s.

The wear intensity I (mg/km) is defined as the ratio between the mass wear of the rock destruction element $\Delta m = m_{in} - m_f$ to the drifting for a tool element L, where m_{in} and m_f (mg) are the sample masses before and after testing, respectively:

$$I = \frac{\Delta m}{L}; \ L = \frac{\pi D n}{60} t,$$

where D is the core diameter, km; n is the rotation frequency of the work spindle, min^{-1}; t is the cutting time, min.

The comparative testing of samples were carried out at a cutting speed of 1.35 m/s, the length of turning 1180 m, turning time 870 s.

RESULTS AND DISCUSSION

Thermal weight loss

The weight loss of CVD diamond, PCD, and UHPCD after thermal treatment are given in Table 1. It is shown that the thermal weight loss of CVD diamond is larger than those of PCD and UHPCD. Furthermore, the weight loss rate of CVD diamond is 25.0 %, which is 25 times bigger than that of the UHPCD. However, little difference can be seen between PCD and UHPCD.

The CVD diamond easily loses weight under high temperature. The first reason: a thermal decomposition of nondiamond phases is happened under high temperature [7]. The other reason: it is supposed that the residual oxygen in the furnace results in oxidation. The early stage of the oxidation process for CVD diamond occurred preferentially at grain boundaries and local defects, due to the substantial amount of sp^2 bonded carbon present. It was reported that the oxidation of sp^2 bonded carbon is much easier than that of sp^3 bonded carbon [8]. The atomic oxygen reacts with CVD diamond at the surface and forms CO and CO_2 products. It means that most oxygen react with diamond at the surface of PCD. At the same time, the sintering agent Si and SiC at the surface of PCD react with oxygen. These products could increase the weight of PCD. Therefore, the weight loss of PCD and UHPCD is lower than that of CVD diamond. Furthermore, the CVD diamond is thoroughly exposed to the environment. It will have more chances to contact with oxygen. Whereas the CVD diamond in UHPCD is surrounded by PCD, the size of the area exposed to oxygen is small. It implies that the UHPCD protects CVD diamond against the effect of oxidation.

Table 1. Thermal weight loss of CVD diamond, PCD and UHPCD

No.	Sample	Weight, mg		Weight loss, mg	Weight loss rate, %
		untreated	thermal treated		
1	PCD	135.2	133.7	1.5	1.1
2	CVD	8.8	6.6	2.2	25.0
3	UHPCD	137.6	136.2	1.4	1.0

Hardness

Table 2 exhibits the hardness of CVD diamond in UHPCD. It can be seen that the CVD diamond has a rather high initial hardness, which is 94±4 GPa. After HP-HT, the hardness of CVD diamond in the UHPCD increases up to 140 GPa. The increasing hardness of the CVD diamond results from the plastic deformation of diamond grains during the formation around CVD diamond [5]. The hardness of the CVD diamond in thermal treated UHPCD decreases from 133±7 GPa to 109±3 GPa while it is still higher than 94±4 GPa of the untreated UHPCD.

Table 2. Hardness of CVD diamond in UHPCD

Hardness of CVD diamond, GPa		
untreated	untreated UHPCD	thermal treated UHPCD
94±4	133±7	109±3

In the structure of diamond, sp^3 orbitals contribute to formation of four C–C bonds, which produce tetrahedral structure of diamond. Hardness of CVD diamond usually varies over a wide range with sp^3 to sp^2 bonding ratio. The bonding ratio depends on the kinetic energy of the carbon species and amount of hydrogen. It was reported that the predominant defects were hydrogen clusters and nondiamond impurity phases for the CVD diamond [9]. These defects usually produce some local strain in the CVD diamond. Therefore, the strain distorts the atomic arrangement in the diamond lattice. Hydrogen clusters or nondiamond phase react with residual oxygen in the furnace, then the defects can be removed. The weakened local strain and more normal atomics in the CVD diamond lattices could be formed. Thus, the hardness of the CVD diamond decreases after the thermal treatment.

Raman spectra

The Raman spectra of the samples exhibited a C–C single-phonon band of vibrations near the 1332 cm^{-1} region, which is characteristic of carbon compounds of the type of diamond with the sp^3 chemical bond hybridization [10]. The full width at half maximum (FWHM, Γ) and wavenumber position (ω) of a Raman line are compared. The FWHM is dependent on many complex factors such as crystallite size or structural disorders [11]. When the crystal is subjected to externally imposed stress or internal flaws caused stress, the position of the Raman peak is subtly affected.

Raman spectra of CVD diamonds (untreated, untreated UHPCD, and thermal treated UHPCD) are given in Table 3. It is shown that the peak position of CVD diamond increases from 1333.3 to 1334.0 cm^{-1} and the FWHM increases from 9.3 to 12.7 cm^{-1} after HPHT treatment. A high value of the FWHM means a heavy disordering of the CVD diamond material. The variations of the peak position and FWHM point to the inhomogeneous distribution of elastic deformations and perfection degree of the crystal structures of diamond. It has been found that the broadened FWHM of the CVD diamond in UHPCD is evidently due to the increase of the structural defect concentration [5].

Table 3. Raman spectra of CVD diamonds

Parameter	CVD diamond	Untreated UHPCD	Thermal treated UHPCD
ω, cm^{-1}	1333.3	1334.0	1332.9
Γ, cm^{-1}	6.4	10.9	6.8

The FWHM of CVD diamond in thermal treated UHPCD becomes narrower than that of CVD diamond in untreated UHPCD. It is closer to natural and synthetic diamond single crystals whose FWHM were only 2–2.5 cm^{-1}[12]. The FWHM reflects the degree of distortion [13]. The distortion in crystallographic symmetry removes the Raman peak completely or partially. The strain weakens after eliminating the defects. Meanwhile the distortion is less. It was reported that a significant reduction of impurity phases in CVD diamond leads to an appreciable reduction of the FWHM of Raman spectra [9]. It can be concluded that the distortion of the CVD diamond in UHPCD becomes weaker after thermal treatment.

The peak position decreases from 1334.0 to 1332.9 cm^{-1} after the thermal treatment. The position of the Raman peak is affected by stress [14]. Compressive stress results in a shift of the peak to higher frequencies, and tensile stress results in

a shift of the peak to lower frequencies. The peak position decreases to 1332.9 cm^{-1}, but it is still higher than the theoretical position 1332.5 cm^{-1}. The results showed that the compressive stress is partly released after thermal treatment. But the crystal in CVD diamond is still subjected to compressive stress. Hydrogen clusters or nondiamond phases usually produce some strain and distort atomic arrangement in the diamond lattice. They are removed after thermal treatment. Then the distortion weakens. The compressive stress is released. Therefore, the peak position is shifted to lower wavenumber.

Wear performances

The wear loss of the untreated and thermal treated UHPCD are shown in Table 4. The average wear rate of the untreated UHPCD is 0.17 mg/km and of thermal treated UHPCD the average wear rate is 0.6 mg/km. The thermal treatment increases the wear loss of UHPCD. The wear resistance of thermal treated UHPCD is better than that of PCD by a factor of 10.

Table 4. Wear loss of the untreated and thermal treated UHPCD

Sample	Sample No.	Weight, mg		Wear loss, mg	Wear rate, mg/km	Average wear rate, mg/km
		initial	final			
Untreated UHPCD	1	133.4	133.2	0.2	0.17	0.17
	2	135.4	135.2	0.2	0.17	
Thermal treated UHPCD	1	130.6	129.8	0.8	0.53	0.60
	2	128.8	127.8	1.0	0.67	
PCD	1	92.6	82.6	10.0	6.10	6.10

Discussion

The hardness of the CVD diamond in UHPCD decreases from 133±7 to 109±3 GPa after thermal treatment. At the same time, the wear resistance of the thermal treated UHPCD is lower than that of the untreated UHPCD. The obtained result is consistent with the result reported in [13]. Even though the CVD diamond in our experiment and the CVD diamond material in [13] were not manufactured in the same factory, they belong to the same kind of superhard materials. Furthermore, there is a quasilinear relationship between the hardness and wear resistance of diamond [15]. The narrowing of FWHM and downshift of Raman peak are consistent with the decrease of hardness and wear resistance of CVD diamond. The growth defects affect the hardness and wear resistance of the UHPCD. Both the crystal structure defects and released compressive stresses in CVD diamond result in the drop of the hardness after thermal treatment. Hydrogen clusters and nondiamond carbon phases are removed under high temperature by thermal decomposition and oxidation. The residual atomic oxygen reacts with hydrogen clusters and nondiamond impurity phases at the surface of CVD diamond. And then these kinds of defects are removed from CVD diamond. The distortion about atomic arrangement in the diamond lattice weakens. The FWHM of Raman spectrum reflects the degree of the crystal structure distortion. The FWHM of CVD diamond is narrower after thermal treatment. It shows a decrease of the structural defects in this material. A shift of the Raman peak is dependent on the stress of the CVD diamond crystal. The strain in diamond lattice weakens after removing the defects. And then the compressive stresses are released. Therefore, the peak position moves to a lower wavenumber. Nevertheless, the UHPCD can be recognized as a kind of materials with excellent heat durability and wear resistant

performance. Based on the research of the UHPCD properties, the material could be recommended for manufacturing drilling bits and dressing tools.

CONCLUSIONS

The following conclusions have been drawn from this study:

– after HPHT the hardness of CVD diamond inside the UHPCD increased by 41 %. Although after the thermal treatment the hardness of CVD diamond decreased from 133±7 to 109±3 GPa, it was still higher than 94±4 GPa that of the untreated UHPCD;

– the lower hardness of the CVD diamond in the thermal treated UHPCD contributed to a higher wear rate. The wear rate of the UHPCD decreased from 0.17 mg/km to 0.6 mg/km after thermal treatment, but it was still much lighter than 6.1 mg/km that of the PCD;

– the narrowing of the FWHM and the downshift of Raman peak were implied the lighter structural defects and released compressive stresses under high temperature, which result in a drop of the hardness and wear resistance of CVD diamond in thermal treated UHPCD.

Досліджено термічну стабільність надтвердого полікристалічного алмазного (UHPCD) композиційного матеріалу, отриманого армуванням полікристалічного алмазу після хімічного осадження (CVD) алмазу в потоці аргону при 1200 °C. Для порівняння твердості, C–C-структури і зносостійкості необробленого та термообробленого UHPCD було досліджено заглиблення індентора, спектри комбінаційного розсіювання та знос. Показано, що твердість CVD-алмазу в UHPCD досягає 133±7 ГПа після дії високого тиску і високої температури, а після термообробки зменшується до 109±3 ГПа, зносостійкість UHPCD після термообробки зменшується від 0,17 до 0,6 мг/км. Звуження напівширини і зсув піку комбінаційного розсіювання в область низьких частот CVD-алмазу в термообробленому UHPCD характеризує зменшення кристалічних структурних дефектів і напружень стиску, що призводить до зниження твердості CVD-алмазу в термообробленому UHPCD. Вища швидкість зносу термообробленого UHPCD пов'язана з більш низькою твердістю.

Ключові слова: надтверді полікристалічні алмази, термостабільність, CVD-алмази, зносостійкість.

Исследована термическая стабильность сверхтвердого поликристаллического алмазного (UHPCD) композиционного материала, полученного армированием поликристаллического алмаза после химического осаждения (CVD) алмаза в потоке аргона при 1200 °C. Для сравнения твердости, C–C-структуры и износостойкости необработанного и термообработанного UHPCD были исследованы глубина проникновения индентора, спектры комбинационного рассеяния и износ. Показано, что твердость CVD-алмаза в UHPCD достигает 133±7 ГПа после действия высокого давления и высокой температуры, а после термической обработки уменьшается до 109±3 ГПа, износостойкость после термической обработки UHPCD уменьшается от 0,17 до 0,6 мг/км. Сужение полуширины и сдвиг пика комбинационного рассеяния в область низких частот CVD-алмаза в термообработанном UHPCD характеризует уменьшение кристаллических структурных дефектов и напряжений сжатия, что приводит к снижению твердости

CVD-алмаза в термообработанном UHPCD. Более высокая скорость износа термически обработанного UHPCD связана с более низкой твердостью.

***Ключевые слова**: сверхтвердые поликристаллические алмазы, термо-стабильность, CVD-алмазы, износостойкость.*

1. *Akaishi M., Yamaoka S., Ueda F., Ohashi T.* Synthesis of polycrystalline diamond compact with magnesium carbonate and its physical properties // Diamond Relat. Mater. – 1996. – **5**, N 1. – P. 2–7.
2. *Ueda F., Ohashi T., Akaishi M., Yamaoka S.* Cutting performance of sintered diamond with $MgCO_3$ as a sintering agent // Mater. Sci. Eng. A. – 1996. – **209**. – P. 260–263.
3. *Akaishi M., Yamaoka S.* Physical and chemical properties of the heat resistant diamond compacts from diamond-magnesium carbonate system // Ibid. – 1996. – **209**. – P. 54–59.
4. *Westraadt J. E., Dubrovinskaia N., Neethling J. H., Sigalas I.* Thermally stable polycrystalline diamond sintered with calcium carbonate // Diamond Relat. Mater. – 2007. – **16**, N 11. – P. 1929–1935.
5. *Shul'zhenko A. A., Ashkinazi E. E., Sokolov A. N. et al.* Novel hybrid ultrahard materialal // J. Superhard Mater. – 2010. – **32**, N 5. – P. 293–300.
6. *Shul'zhenko A. A., Sokolov A. N., Loshak M. G. et al.* Physico-mechanical properties and structure of diamond polycrystalline composite materials produced from variously dispersed powders // Ibid. – 2008. – **30**, N 1. – P. 23–27.
7. *Obraztsov A. N., Kopylov P. G., Chuvilin A. L., Savenko N. V.* Production of single crystal diamond needles by a combination of CVD growth and thermal oxidation // Diamond Relat. Mater. – 2009. – **18**. – P. 1289–1293.
8. *Pu J. C., Wang S. F., Sung J. C.* High-temperature oxidation behaviors of CVD diamond films // Appl. Surf. Sci. – 2009. – **256**. – P. 668–673.
9. *Chen K. H., Lai Y. L., Chen L. C. et al.* High-temperature Raman study in CVD diamond // Thin Solid Films. – 1995. – **270**. – P. 143–147.
10. *Ralchenko V., Nistor L., Pleuler E. et al.* Structure and properties of high-temperature annealed CVD diamond // Diamond Relat. Mater. – 2003. – **12**. – P. 1964–1970.
11. *Fortunato W., Chiquito A. J., Galzerani J. C., Moro J. R.* Crystalline quality and phase purity of CVD diamond films studied by Raman spectroscopy // J. Mater. Sci. – 2007. – **42**, N 17. – P. 7331–7336.
12. *Miyamoto M., Takse T., Mitsuda Y.* Raman spectra of various diamonds // Mineral. J. – 1993. – **16**, N 5. – P. 246–257.
13. *Sokolov A. N., Shul'zhenko A. A., Gargin V. G. et al.* Structure and physico-mechanical properties of CVD diamonds of various crystalline perfections in the Hybridite material // J. Superhard Mater. – 2013. – **35**, N 2. – P. 83–92.
14. *Huang E. P., Huang E., Yu S. C. et al.* High-temperature and pressure Raman spectroscopy of diamond // Materials Letters. – 2010. – **64**. – P. 589–582.
15. *Domsa S.* Predicting the wear resistance of diamond tools matrices via composition/hardness // Diamond Tool. Proc. – 2002. – P. 57–62.

School of Engineering and Technology,
China University of Geosciences, Beijing

Key Laboratory of Deep Geo-drilling Technology
of the Ministry of Land and Resources, China University of Geosciences, Beijing

Beijing Huayou Guanchang Environment
and Energy Science & Technology Development Co., LTD, Beijing, China